Eur Biophys J (2010) 39:1229–1242
DOI 10.1007/s00249-010-0576-0

ORIGINAL PAPER

Effects of dithiothreitol on the amyloid fibrillogenesis of hen egg-white lysozyme

Steven S.-S. Wang · Kuan-Nan Liu · Bo-Wei Wang

Received: 5 April 2009 / Revised: 3 December 2009 / Accepted: 13 January 2010 / Published online: 7 February 2010

Abstract At least 25 human proteins can fold abnormally to form pathological deposits that are associated with several degenerative diseases. Despite extensive investigation on amyloid fibrillation, the detailed molecular mechanisms remain rather elusive and there are currently no effective cures for treating these amyloid diseases. The present study examined the effects of dithiothreitol on the fibrillation of hen egg-white lysozyme (HEWL). Our results revealed that the fibrillation of hen lysozyme was significantly inhibited by reduced dithiothreitol (DTT^{red}) while oxidized dithiothreitol (DTT^{ox}) had no anti-aggregating activity. Effective inhibitory activity against hen lysozyme fibrillation was observed only when DTT^{red} was added within 8 days of incubation. Our results showed that the initial addition of DTT^{red} interacted with HEWL, leading to a loss in conformational stability. It was concluded from our findings that DTT^{red}-induced attenuation of HEWL fibrillation may be associated with disulfide disruption and extensive structural unfolding of HEWL. Our data may contribute to rational design of effective therapeutic strategies for amyloid diseases.

Keywords Lysozyme · Amyloid fibril · Reductant · Dithiothreitol · Inhibition · Disulfide bond

Introduction

Protein aggregation is of enormous importance in a broad range of disciplines, including biochemical research, the biotechnology industry, and human pathology. In general, protein aggregates can be considered as insoluble multimeric proteins that have lost their native forms and functions. Aggregation of proteins is a nuisance in applications in the biopharmaceutical industry, where it can interfere with production and characterization of therapeutic proteins/peptides (De Bernardez Clark 2001; Morozova-Roche and Malisauskas 2007; Singh and Panda 2005). On the other hand, protein aggregation, especially amyloid fibrillation, underlies a vast array of debilitating human diseases, collectively know as conformational diseases. Among these are hemodialysis amyloidosis, type II diabetes, Parkinson's disease, Huntington's disease, and Alzheimer's disease (Chiti and Dobson 2006; Ross and Poirier 2004; Uversky and Fink 2004; Wang and Good 2005).

Various proteins associated with the above-mentioned conformational diseases have been identified to possess amyloid-forming ability in vivo (Bennett 2005; Goedert and Spillantini 2006; Lee et al. 2001). While these disease-associated amyloidogenic proteins differ in their sequence, structure, and function, they all form similar, highly ordered amyloid fibrils exhibiting several morphological and histochemical staining properties in common, for example, exhibition of cross-β structure motif, fibrillar morphology, birefringence upon staining with aromatic dye Congo red, protease resistance, and insolubility in most solvents (Dobson 2004; Lansbury 1999; Ross and Poirier 2004; Serpell et al. 2000; Uversky and Fink 2004; Wang and Good 2005). Moreover, recent findings suggest that amyloid fibrillation is also possible with proteins that are irrelevant to any known amyloid disease under certain conditions in vitro (Chiti and Dobson 2009; Ferrao-Gonzales et al. 2000; Lai et al. 1996; Shtilerman et al. 2002; Wang 2005). These observations

S. S.-S. Wang (✉) · K.-N. Liu · B.-W. Wang
Department of Chemical Engineering, National Taiwan University, No. 1, Sec. 4, Roosevelt Road, Taipei 10617, Taiwan
e-mail: sswang@ntu.edu.tw

have led to the concept that the ability to form amyloid fibril might be considered as a merely generic property of polypeptide chains (Chiti and Dobson 2009; Dobson 2004; Fandrich et al. 2003; Kallberg et al. 2001; Ross and Poirier 2004; Taylor et al. 2002; Uversky and Fink 2004). By taking advantage of this generic property, investigation of amyloid fibrillation using non-disease-associated proteins can thus aid in our understanding of possible inhibition of amyloid aggregation.

While amyloid-related diseases have been at the center of intense research efforts, no effective cure is currently being directed toward treating the diseases. The reduction of amyloid fibrillation and the capture of fibrillar species have been widely viewed as effective approaches to tackling amyloidoses. Considerable efforts have been devoted to developing or seeking anti-aggregating or anti-amyloidogenic agents as potential strategies to fight amyloidoses (Estrada and Soto 2007; Gazova et al. 2008; Porat et al. 2006).

Hen egg-white lysozyme (HEWL) is a 129-amino-acid-long enzyme used to catalyze the hydrolysis of the β-linkage between *N*-acetylmuramic acid and *N*-acetylglucosamine subunits in the peptidoglycan polymers of many bacterial cell walls and then lyse bacteria. Its native form is cross-linked by four disulfide bonds and adopts mainly helical conformation ($\sim$30% α-helix, $\sim$6% β-sheet) (Vaney et al. 1996). HEWL is one of the best characterized and most studied of all proteins. HEWL is one of the widely studied food proteins and its three-dimensional structure, folding–unfolding mechanism, unfolding intermediates, and stability information have been extensively characterized (Frare et al. 2004; Krebs et al. 2000; Mishra et al. 2007). Furthermore, HEWL is structurally homologous to human lysozyme ($\sim$60% sequence homology), which has been found to be responsible for hereditary nonneuropathic systemic amyloidosis (Booth et al. 1997; Pepys et al. 1993). Therefore, given the aforesaid features, HEWL serves as an ideal model system to study in vitro fibrillation.

In this research, using HEWL as a model system to induce fibrillation, we set out to investigate the effects of reduced dithiothreitol (DTT^{red}) on the aggregating and fibrillogenic behaviors of hen egg-white lysozyme and further characterized the relationship between the presence of DTT^{red} and abnormal protein aggregation resulting in eventual amyloid formation. Via several spectroscopic techniques and electron microscopy, our results showed that HEWL fibrillogenesis was significantly attenuated by DTT^{red}, whereas no antifibrillogenic activity was detected with only oxidized DTT (DTT^{ox}) present. The addition of DTT^{ox} did not affect the inhibitory potency of DTT^{red} when HEWL was incubated with both DTT^{red} and DTT^{ox}. Equilibrium urea-unfolding data revealed that DTT^{red} decreased the stability of HEWL. Moreover, DTT^{red} at 2 mM was found to be effective in reducing HEWL fibrillation when DTT^{red} was added within $\sim$8 days of incubation. As inferred from our data, by further destabilizing the partially unfolded monomer and/or oligomeric nucleus species, DTT^{red} drove the reaction to proceed through the off-pathway toward the formation of amorphous aggregates, and thus a significantly reduced amount of fibrils was detected. Along with free thiol measurements, our findings suggested that reductive environments aid in suppressing amyloid fibrillation of disulfide-bonded proteins. Furthermore, the attenuated fibrillation of HEWL induced by DTT^{red} might be correlated with disulfide disruption and extensive structural unfolding of HEWL. We believe the outcome from this work may not only help decipher the molecular mechanism of amyloid fibrillation but also shed light on rational design of potential therapeutic strategies for amyloid pathology.

Materials and methods

Chemicals and proteins

Hen egg-white lysozyme (HEWL; EC 3.2.1.17) was purchased from Merck (Germany) and used without further purification. Hydrochloric acid, potassium dihydrogen phosphate, sodium chloride, and potassium chloride were purchased from Nacalai Tesque, Inc. (Japan). Reduced dithiothreitol (DTT^{red}), oxidized dithiothreitol (DTT^{ox}), and tris-(hydroxymethyl) aminomethane were purchased from Sigma (USA). All other chemicals, unless otherwise specified, were obtained from Sigma (USA).

Lysozyme sample solution preparation

Sample solutions of 2 mg/mL HEWL were prepared by dissolving 0.1 g lyophilized HEWL in 50 mL hydrochloric acid with salt (136.7 mM NaCl, 2.68 mM KCl, pH 2.0) with 0.01% (w/v) sodium azide. HEWL sample solutions were first mixed via vortexing and then incubated at 55°C to induce fibrillar species.

Thioflavin T fluorescence assay

Forty microliters of HEWL samples taken at different times were mixed with 960 μL 10 μM thioflavin T (ThT) in phosphate-buffered saline (PBS) with 0.01% (w/v) sodium azide. ThT fluorescence intensity measurements were performed by exciting samples at 440 nm and recording emission intensities at 485 nm using a F-2500 fluorescence spectrophotometer (Hitachi, Japan).

Congo red binding assay

To assess the presence of amyloid fibrils in the HEWL solutions, Congo red binding studies were performed. Congo red dye was dissolved in PBS to final concentration of 112 μM. Congo red absorbances of HEWL sample solutions were determined by adding Congo red to a final concentration of 20 μM and acquiring spectral measurements from 400 to 700 nm at 25°C on a Spectronic Genesys 5 spectrophotometer (Spectronic Instrument, USA). All HEWL sample solutions were allowed to interact with Congo red for at least 30 min prior to recording their spectra.

Circular dichroism spectroscopy

Circular dichroism (CD) spectra of HEWL samples were recorded on a JASCO J-715 (150-S type) spectrometer (Jasco, Japan) at 25°C using a bandwidth of 2.0 nm, a step interval of 0.1 nm, and an averaging time of 2 s. A 1-mm quartz cell was used for far-ultraviolet (far-UV; 190–260 nm) measurements. Three scans each of duplicate samples were measured and averaged. Control buffer scans were run in duplicate, averaged, and then subtracted from the sample spectra. The results were plotted as ellipticity (mdeg) versus wavelength (nm).

Anilinonaphthalene-8-sulfonic acid (ANS) binding

Hundred-microliter HEWL sample solutions were mixed with 900 μL ANS working solution of 20 μM, and then the mixtures were incubated in the dark for 30 min at room temperature. ANS fluorescence intensities were recorded by exciting samples at 380 nm, and emissions were recorded between 420 and 580 nm on a F-2500 fluorescence spectrophotometer (Hitachi, Japan). All measurements were repeated at least three times. The representative ANS fluorescence intensity was taken at the average emission wavelength (AEW), which accounts for both changes in intensity and spectrum envelope. The determination of AEW was carried out using the following equation:

$$\mathrm{AEW} = \frac{\sum (F_i \times \lambda_i)}{\sum F_i},$$

where F_i is the ANS fluorescence intensity at wavelength λ_i.

Right-angle light scattering

The scattered light intensities (at a fixed angle of 90°) were detected in the HEWL samples on a F-2500 fluorescence spectrophotometer (Hitachi, Japan) at equal excitation and emission wavelengths of 450 nm.

Equilibrium unfolding measurement and data analysis

Both the stock solutions of HEWL with 0, 1, 2, and 4 mM DTT^{red} and 10 M urea were dissolved in hydrochloric acid with 136.7 mM NaCl, 2.68 mM KCl, and 1.54 mM NaN_3 (pH ~2.0). The two stock solutions were mixed in different ratios to prepare sample solutions with urea concentrations ranging from 0 to 9 M. The HEWL sample–denaturant solutions were incubated at 25°C until reaching equilibrium before measuring their intrinsic tryptophan fluorescence intensities. All fluorescence measurements were taken by exciting sample solutions at 280 nm, with fluorescence emission spectra collected from 300 to 400 nm. The obtained urea-induced unfolding data were fitted to a two-state transition model mechanism described below.

For the two-state transition model mechanism, the free energy change of unfolding of HEWL ($\Delta G_{\mathrm{unfold}}$) and the equilibrium constant for unfolding (K_{unfold}) at any used denaturant concentration can be determined via the following equation:

$$\begin{aligned}\Delta G_{\mathrm{unfold}} &= \Delta G^0_{\mathrm{unfold}} - m_{\mathrm{unfold}}[\mathrm{urea}] = -RT\ \ln(K_{\mathrm{unfold}}) \\ &= -RT\ \ln\left(\frac{f}{1-f}\right) = -RT\ \ln\left(\frac{F_{\mathrm{fold}} - F}{F - F_{\mathrm{unfold}}}\right),\end{aligned}$$

where $\Delta G^0_{\mathrm{unfold}}$ is the free energy change of unfolding in water obtained from linear extrapolation to 0 M urea, f is the fraction of unfolded HEWL at various urea concentrations, F is the fluorescence of HEWL at any urea concentration, F_{fold} and F_{unfold} are the fluorescence intensities of HEWL in the folded and the unfolded states, respectively, which are assumed to be linearly dependent on the urea concentration, and m_{unfold} is the slope of the transition obtained by the method of least-squares analysis in the transitional urea concentration region. Aside from $\Delta G^0_{\mathrm{unfold}}$, we also used the midpoint concentration of the denaturant curve (C_m), i.e., the denaturant concentration at which half of proteins were unfolded ($\Delta G_{\mathrm{unfold}} = 0$), as another measure of stability.

Detection of free thiol groups of HEWL

Free thiol groups were detected with the Ellman assay upon reaction with 5,5′-dithio-bis-2-nitrobenzoic acid (DTNB). An excess of DTNB (1,000 μL) (DTNB stock solution at concentration of 2.2 mM) was added to 1,000 μL HEWL solution. The concentration of free thiol groups was determined with DTNB using absorbance at 412 nm and a molar extinction coefficient of 13,784 $M^{-1}\ cm^{-1}$ for 5-thio-2-nitrobenzoic acid (TNB).

Transmission electron microscopy

Ten microliters of HEWL sample was placed on carbon-stabilized formvar-coated grids. Grids were negatively

stained with 2% (w/v) aqueous uranyl acetate (Electron Microscopy Sciences, USA) and then examined and photographed in a H-7650 transmission electron microscope (Hitachi, Japan) at an accelerating voltage of 75 kV.

Statistical analysis

All data represent mean ± standard deviation (SD) for n independent determinations. Significance of results was determined by Student's t test on n independent measurements, where n is specified in the figure legend. Unless otherwise indicated, significance was taken as $P < 0.005$.

Results and discussion

To study the influence of the reduced form of DTT on amyloid fibril formation of HEWL, we initially added DTT^{red} to HEWL solutions and monitored the changes of ThT fluorescence emissions and Congo red binding spectra of HEWL samples. Thioflavin T (ThT) is believed to interact specifically and rapidly with amyloid fibrils, and an elevation in ThT fluorescence signal has been considered as an important indicator of the presence of amyloid fibril (LeVine 1993). As seen in Fig. 1, the ThT fluorescence emission of HEWL itself increased dramatically in the first 10 days, and then reached a fluorescence plateau after 20 days of incubation. However, when DTT^{red} was added to the sample solution, a considerable reduction in ThT fluorescence emission was observed, spanning over 50 days, implying that amyloid fibrillation of HEWL was considerably suppressed by the addition of DTT^{red}. Moreover, the percentage reduction of ThT fluorescence induced by DTT^{red} was found to be ~80–90%.

As a complementary measure of the presence of amyloid fibril, Congo red binding to HEWL samples was performed. We show in Fig. 2a and b that HEWL by itself significantly bound Congo red and shifted the spectral properties of Congo red binding. An increase in Congo red absorption accompanied by a red-shift of the spectral maximum was

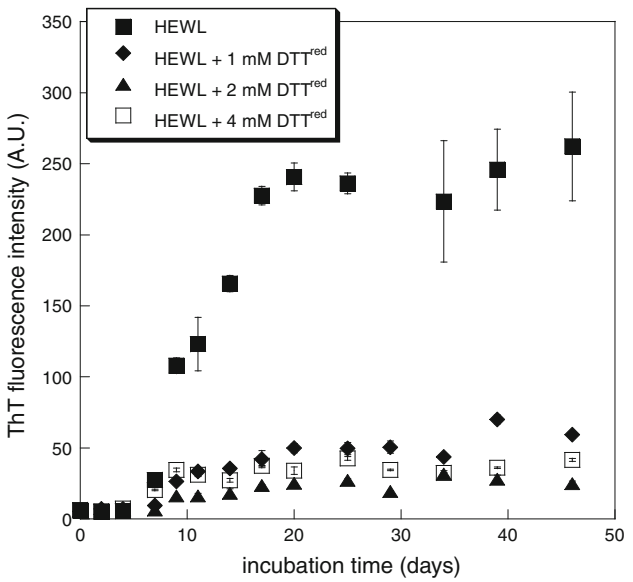

Fig. 1 Effect of DTT^{red} on amyloid fibrillation of HEWL as a function of time. Extent of fibril formation was measured via ThT fluorescence emission. Each *point* represents the average of at least five independent measurements ($n \geq 5$). HEWL samples were prepared in hydrochloric acid (pH 2.0) with salt in the presence of various concentrations of DTT^{red} (1, 2, and 4 mM), and incubation was performed at 55°C

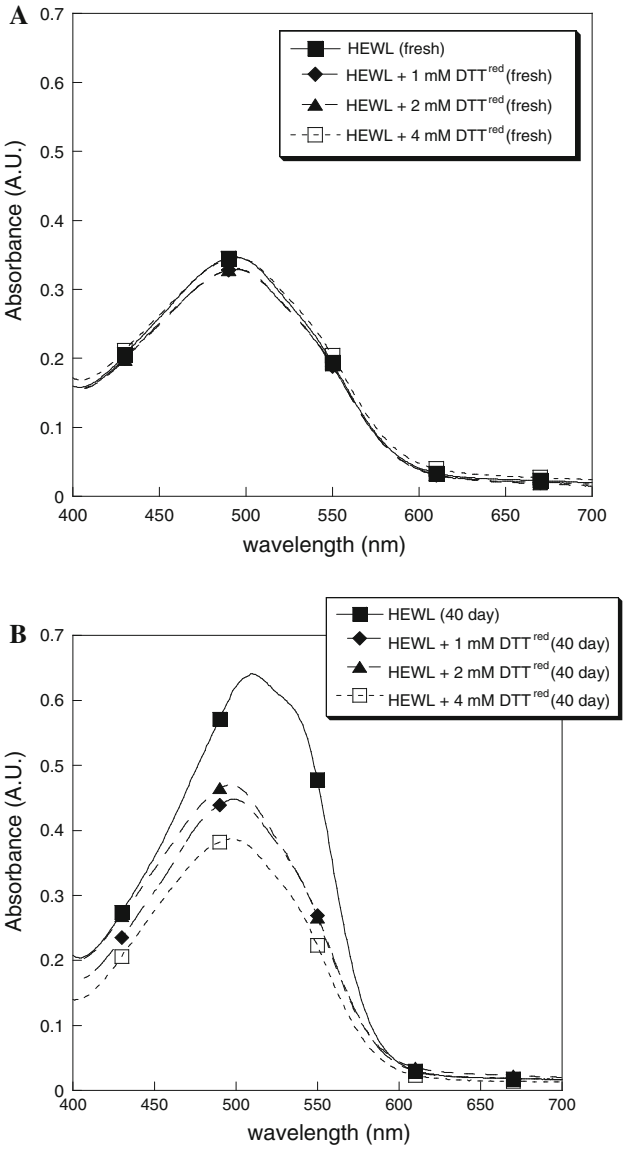

Fig. 2 Representative Congo red binding spectra of HEWL samples taken at **a** 0 days and **b** 40 days of incubation. HEWL samples were prepared in hydrochloric acid (pH 2.0) with salt in the presence of various concentrations of DTT^{red} (0, 1, 2, and 4 mM), and incubation was performed at 55°C

observed during incubation. On the contrary, due to the lack of a shoulder peak at ~540 nm in the Congo red absorbance spectra, no appreciable amount of amyloid fibril was observed in the HEWL sample with 4 mM DTT^{red} even after 40 days of incubation, signifying a notable loss in amyloid fibril content. Hence, our ThT fluorescence and Congo red binding results suggested that fibril formation was retarded by the presence of reductant (DTT^{red}).

Further confirmation of suppression of HEWL fibrillation by DTT^{red} came from the transmission electron micrographs of HEWL with and without DTT^{red} present in the sample solution (Fig. 3a, b). As seen in Fig. 3a, after 30 days of incubation, HEWL itself formed a high density of long individual fibrils and sheet-like structures with larger cross-sectional area composed of fibril bundles. However, exposure to DTT^{red} resulted in remarkable attenuation of HEWL fibrillation and considerably reduced the amount of HEWL fibrils [see Fig. 3b for HEWL-DTT^{red} (4 mM) mixture]. Our preceding results suggested that superior anti-amyloidogenic activity against HEWL fibrillation was exhibited by DTT^{red}.

It has previously been reported that, by varying external factors, conformational variations can be induced leading to potentially different aggregation pathways that result in supramolecular aggregates with different structures (i.e., ordered fibrils and amorphous aggregates) (Powers and Powers 2008; Vetri et al. 2007). Decreased ThT fluorescence signal and formation of fewer fibrils were observed in DTT^{red}-treated HEWL samples (Figs. 1, 3), which may arise from competition between the fibrillation pathway (on-pathway) and the amorphous aggregation pathway (off-pathway). In order for proteins to form ordered structures such as amyloid fibrils, amorphous aggregation should be suppressed. Also, examination of the relative kinetics of fibrillation and amorphous aggregation of HEWL is important to elucidate the possible mechanism of DTT^{red} inhibitory activity against HEWL fibrillation. To address this issue, the extent of HEWL aggregation as a function of DTT^{red} was evaluated by monitoring the scattered light intensity (both excitation and emission at 450 nm) of the HEWL sample solutions. Right-angle light scattering in a region far from the absorption band at 450 nm has been reportedly used to probe the kinetics of accumulation of aggregates (including fibrillar and non-fibrillar species) (Bliznyukov et al. 2005; Chen et al. 2002; Kells et al. 1984; Thakur and Rao 2008; Zhu et al. 2002), which in theory should reveal the total amount of aggregates formed in the HEWL samples. We show in Fig. 4 that the scattered light intensity of HEWL by itself (the control) increased with prolonging incubation time. Moreover, HEWL samples with DTT^{red} evidently exhibited a comparable scattered light intensity level relative to that of the control, indicating that the addition of DTT^{red} induced the formation of larger aggregates that scattered light. However, these aggregated species formed in the DTT^{red}-containing samples did not bind strongly to ThT, as can be seen from its low final ThT fluorescence intensity shown in Fig. 1, suggesting that the enhanced light scattering in the HEWL samples with DTT^{red} came from the generation of amorphous non-amyloid-like aggregates. This point was also confirmed by our TEM observation (Fig. 3b).

To understand the role that DTT^{red} plays in the structural changes of HEWL, far-UV circular dichroism spectra of HEWL samples were measured. Initially, the far-UV CD spectra of HEWL samples both with and without inhibitors all displayed a similar spectrum, with a shoulder at ~225 nm and an absorption minimum at ~208 nm,

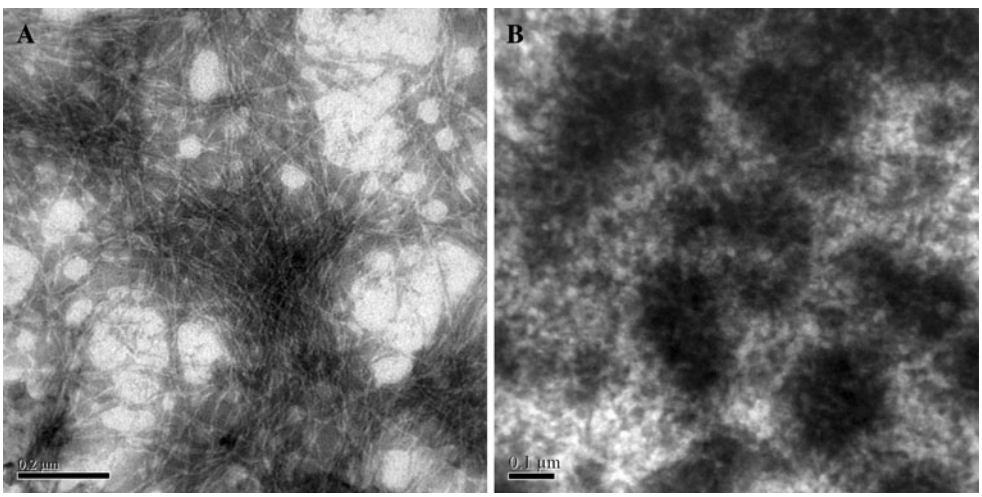

Fig. 3 Electron micrographs of negatively stained HEWL: **a** by itself after 30 days of incubation, **b** co-incubated with 4 mM DTT^{red} after 30 days of incubation (bar = 0.2 μm)

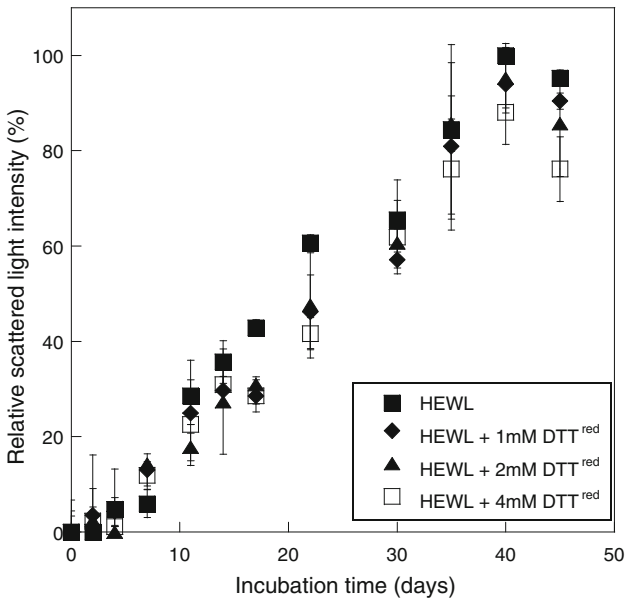

Fig. 4 Kinetics of aggregate formation in HEWL samples with or without DTT^{red}. Extent of aggregation was evaluated by monitoring the scattered light intensity of the HEWL sample solutions at equal excitation and emission wavelengths of 450 nm. Each *point* represents the average of at least five independent measurements ($n \geq 5$). HEWL samples were prepared in hydrochloric acid (pH 2.0) with salt in the presence of various concentrations of DTT^{red} (0, 1, 2, and 4 mM), and incubation was performed at 55°C

reflecting an α-helix-rich conformation ($\sim$37%) (Fig. 5a). Nevertheless, after incubation for $\sim$43 days, occurrence of α-to-β transition along with prominent alteration in the relative proportion of secondary structures within the solution was detected for HEWL alone (ratio of α-helix to β-sheet content: from 2.31 to 0.09). The CD spectra obtained from HEWL by itself were observed to possess a characteristic pattern of β-sheet-rich conformation, and the β-sheet content was significantly raised up to twofold in the fibrillar HEWL samples. Conversely, as shown in Fig. 5b, upon prolonged incubation (e.g., $\sim$43 days), a variation in the shape of CD spectra in which a pronounced absorption minimum occurred in the vicinity of $\sim$200 nm was detected upon the addition of DTT^{red}, indicating that the essentially unordered polypeptide species with higher proportion of random coil structure were observed in DTT^{red}-containing HEWL samples (1 mM DTT^{red}: 53%, 2 mM DTT^{red}: 45%, 4 mM DTT^{red}: $\sim$59%). Our data also revealed that the presence of DTT^{red} markedly attenuated the content of β-sheet detected in the control (0 mM DTT^{red}: $\sim$33%, 1 mM DTT^{red}: $\sim$25%, 2 mM DTT^{red}: $\sim$31%, 4 mM DTT^{red}: $\sim$13%).

In exploring the effect of DTT^{red} on the change in tertiary structure of HEWL, in particular surface hydrophobicity, we recorded the time evolution of ANS fluorescence emission spectra of HEWL samples. ANS is an aromatic, hydrophobic, charged fluorescent probe. Changes in ANS fluorescence have frequently been used to probe for the partially folded conformation of intermediate species such as globular proteins. The intermediate species are characterized by the presence of solvent-exposed hydrophobic clusters (Liu et al. 2005; Rodionova et al. 1989; Semisotnov et al. 1991; Sirangelo et al. 1998; Smoot et al. 2001). The preferential binding of ANS to hydrophobic clusters gives rise to an enhancement in fluorescence emission accompanying a blue-shift of the spectral maximum (Liu et al. 2005; Semisotnov et al. 1991; Smoot et al. 2001). However, ANS generally exhibits weak binding affinity to the native and unfolded state(s) of protein (Dabora et al. 1991; Srisailam et al. 2003). Figure 5c presents the time-dependent variations of ANS fluorescence emission upon addition of DTT^{red}. The surface hydrophobicity of fresh HEWL with or without DTT^{red} was found to be remarkably low, owing to the fact that the hydrophobic site groups are hidden inside the native protein with compactly folded structure. The incubation of HEWL by itself brought about a pronounced enhancement in ANS fluorescence intensity suggestive of the formation of more solvent-exposed hydrophobic regions in HEWL, which probably resulted from conformational changes in the protein leading to partial loss of tertiary structure. However, the addition of DTT^{red} led to a considerably lower ANS fluorescence intensity in comparison with the control (HEWL alone) ($P < 0.005$), as depicted in Fig. 5c. Our ANS fluorescence result is in agreement with the one found in an earlier work (Kumar et al. 2008). We speculate that the reduction in ANS fluorescence intensity may result from the absence of hydrophobic clusters (partially folded structure) and/or the presence of the native or unfolded conformation.

To gain insights into the effect of DTT^{red} on conformational changes in HEWL, intrinsic fluorescence spectra of the samples were also recorded (spectra not shown); the wavelengths of emission maximum (λ_{max}) of all HEWL samples are listed in Table 1. Prolonged incubation led to a slight red-shift of λ_{max} from $\sim$336 to $\sim$339 nm in HEWL fibrillar sample, implying that tryptophan residues were exposed upon fibrillation. However, the λ_{max} of the HEWL samples were shifted toward longer wavelength when DTT was added, and the largest red-shift in λ_{max} was found at 4 mM DTT (from $\sim$336 to $\sim$346 nm), clearly indicative of extensive exposure of tryptophan residues to solvent due to the presence of DTT^{red}.

As evidenced by ANS fluorescence and intrinsic fluorescence results (Fig. 5c, Table 1), the addition of DTT^{red} to HEWL samples during incubation led to obvious structural unfolding of HEWL followed by structural rearrangement through the pathway that resulted in the formation of amorphous aggregated species (as evidenced by an increase in right-angle light scattering in Fig. 4, ThT fluorescence

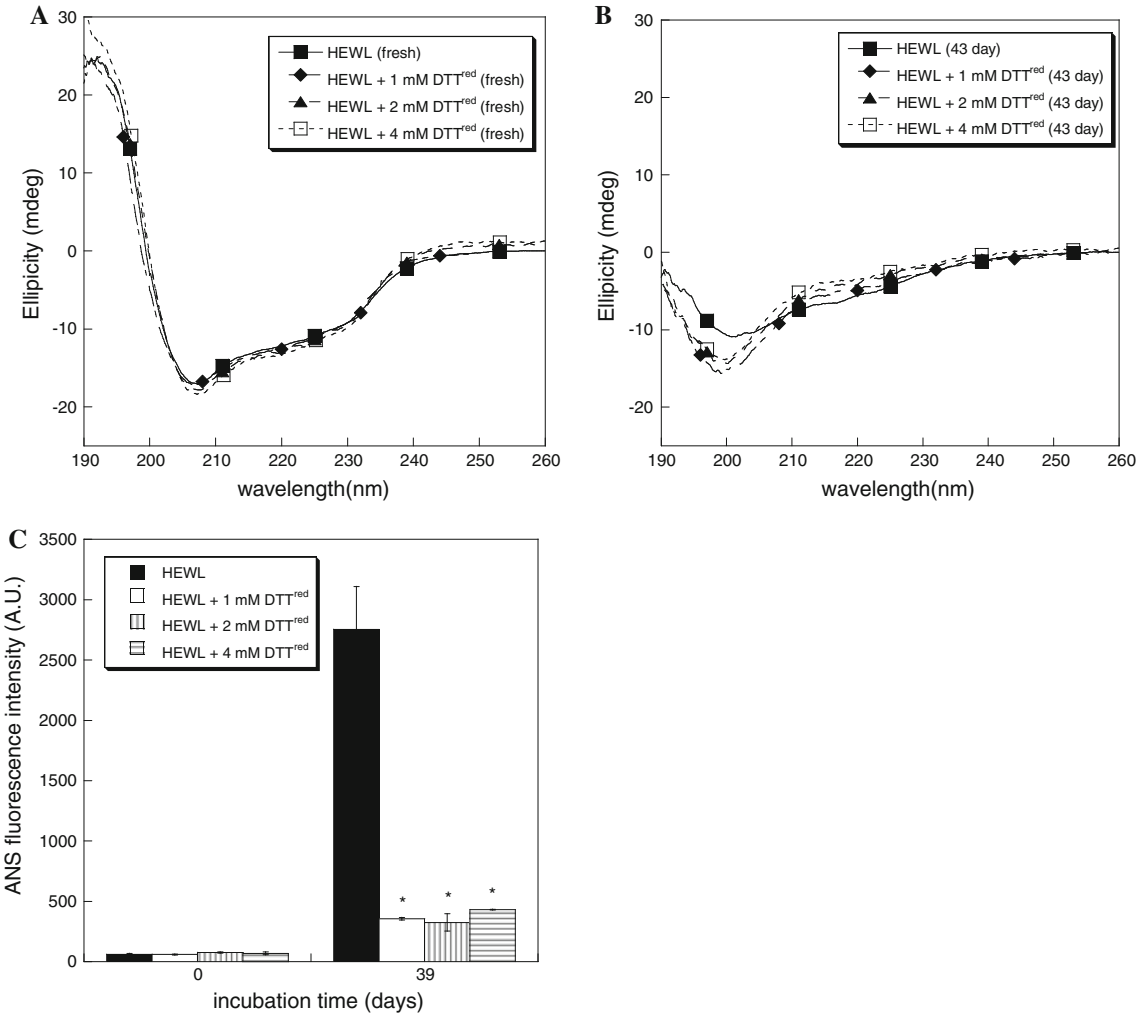

Fig. 5 Influence of DTT^{red} on the secondary structure and surface hydrophobicity of HEWL. **a** Representative circular dichroism spectra of HEWL incubated with various concentrations of DTT^{red} (0, 1, 2, and 4 mM) at 55°C taken at 0 days. **b** Representative circular dichroism spectra of HEWL incubated with various concentrations of DTT^{red} (0, 1, 2, and 4 mM) at 55°C taken at 43 days of incubation. **c** ANS fluorescence emission intensity of HEWL sample as a function of incubation time. ANS fluorescence emission was used to monitor the surface hydrophobicity of HEWL samples. Each *point* represents the average of at least five independent measurements ($n \geq 5$). HEWL samples were prepared in hydrochloric acid (pH 2.0) with salt in the presence of various concentrations of DTT^{red} (0, 1, 2, and 4 mM), and incubation was performed at 55°C. In Fig. 5c, an *asterisk* above the *bar* indicates that the statistical difference between the sample value and its untreated control value has a P value of <0.005 as determined by Student's t test

Table 1 Wavelengths of fluorescence emission maximum of HEWL samples with various concentrations of reduced DTT

$[DTT^{red}]^b$ (mM)	λ_{max} (nm)[a]				
	0 days	9 days	20 days	29 days	39 days
0	336.33	339.33	341.00	341.67	339.33
1	336.00	343.00	343.67	345.33	344.00
2	336.67	343.67	345.33	346.33	345.33
4	336.33	343.33	347.33	347.67	346.33

[a] λ_{max} is the wavelength of fluorescence emission maximum

[b] DTT^{red} is reduced DTT

data in Fig. 1, and TEM results in Fig. 3b). As more of the amorphous aggregates formed, less fibrils were produced, which may explain the positive correlation between treatment with DTT^{red} and attenuation of HEWL fibrillation.

To explore the effects of DTT^{red} on the conformational stability of HEWL at pH 2.0, urea-induced unfolding transitions of HEWL samples in the presence and absence of DTT^{red} (1, 2, or 4 mM) at pH 2.0 were measured using intrinsic fluorescence; the spectral results for HEWL by itself are shown in the inset to Fig. 6. Incubation with urea led to structure unfolding of HEWL and resulted in

energy transfer from the tryptophan residues to a hydrophilic environment, which is manifested as a red-shift of intrinsic fluorescence spectrum from the emission maximum (λ_{max}) of ~340 to ~355 nm. While the fluorescence intensity decreased slightly when the urea concentration fell below 2.5 M (from ~296 to ~267 A.U.), a dramatic increase in fluorescence intensity (from ~267 to ~482 A.U.) and a significant change in λ_{max} were observed when the urea concentration was above 2.5 M. As for the sample with added DTT^{red}, a higher level of fluorescence intensity and pronounced changes in λ_{max} were detected as compared with the control, indicating that the addition of DTT^{red} tended to render the HEWL's conformation more unfolded or flexible, thus leading to its structural instability.

Fitting of the urea-induced transition data for HEWL samples with and without DTT^{red} to the two-state transition model equation (described in the "Materials and methods" section) yielded the dependence of the normalized fraction of unfolded HEWL on urea concentration depicted in Fig. 6. Taken together, the previous findings and the current results reveal that, regardless of the pH and temperature used, the denaturant-induced unfolding process of HEWL can be effectively approximated by a two-state transition under most conditions (Privalov 1996). Also,

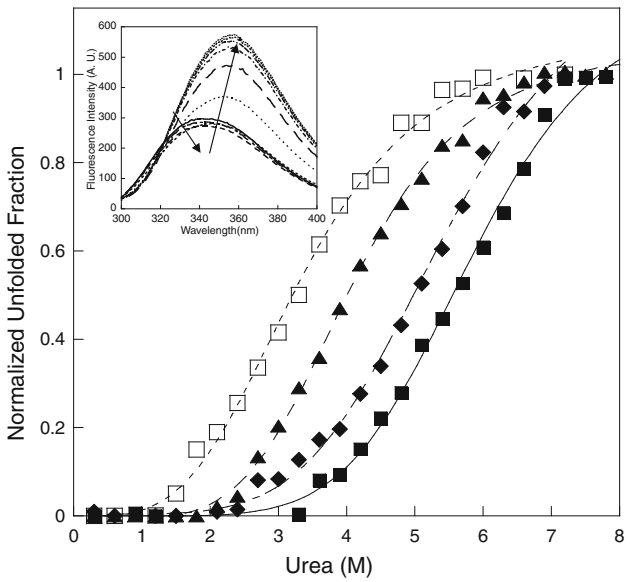

Fig. 6 Urea-induced unfolding transition curves of HEWL monitored by fluorescence spectra in presence and absence of DTT^{red} at pH 2.0 and 55°C. The normalized unfolded fraction of HEWL sample at given urea concentration was determined via a two-state transition model described in the "Materials and methods" section. The concentrations of DTT^{red} used are 0 mM (*filled squares*), 1 mM (*filled diamonds*), 2 mM (*filled triangles*), and 4 mM (*open squares*). The inset shows the intrinsic fluorescence spectra of HEWL at various urea concentrations (the *left arrow* indicates 0–2.5 M and the *right arrow* indicates urea concentrations from 2.5 to 9 M)

we show in Fig. 6 that, upon the addition of urea, our thermodynamic equilibrium experiments demonstrated sigmoidal curves characteristic of cooperative two-state transition during the unfolding of HEWL samples with or without DTT^{red}. Further analysis revealed that the unfolding transition for HEWL without DTT^{red} was observed to fall within the range of ~4–6 M urea, and this concentration range of the unfolding transition was shifted to the left (i.e., to lower urea concentrations) upon exposure to DTT^{red} (HEWL + 1 mM DTT^{red}: ~3–5.5 M, HEWL + 2 mM DTT^{red}: ~2.7–5.0 M, HEWL + 4 mM DTT^{red}: ~1.8–4.0 M), indicating that DTT^{red} did reduce the apparent stability of HEWL.

The values of ΔG^0_{unfold}, m_{unfold}, and C_m were also determined and are listed in Table 2. The magnitudes of ΔG^0_{unfold}, m_{unfold}, and C_m for the unfolding of HEWL by itself were determined to be 17.25 ± 0.48 kJ/mol, 3.09 ± 0.09 kJ/mol-M, and 5.59 ± 0.04 M, respectively. As compared with the published results (Ahmad et al. 1994; Greene and Pace 1974; Nakatani et al. 2007; Sasahara et al. 2002), a reduction in ΔG^0_{unfold} for HEWL in this study was attributed to the structural destruction of HEWL by the condition of lower pH and elevated temperature. While a similar level of m_{unfold} was observed for all HEWL samples, the values of ΔG^0_{unfold} and C_m were found to decrease with increasing concentration of DTT^{red} added (e.g., from 15.13 ± 0.57 kJ/mol and 4.97 ± 0.05 M for HEWL + 1 mM DTT^{red} to 10.12 ± 0.16 kJ/mol and 3.26 ± 0.02 for HEWL + 4 mM DTT^{red}). Two quantities, $\Delta\Delta G^m_{unfold}$ and $\Delta\Delta G^0_{unfold}$, were calculated and used to further compare stability between samples with and without DTT^{red}. $\Delta\Delta G^m_{unfold}$ could be determined via $\Delta\Delta G^m_{unfold} = \langle m \rangle \Delta C_m$, where $\langle m \rangle$ is the average value of m from different sample conditions and ΔC_m is the difference in C_m between HEWL alone and HEWL with DTT^{red}. $\Delta\Delta G^0_{unfold}$ denotes the difference in ΔG^0_{unfold} between HEWL and HEWL-DTT^{red} solution. As shown in Table 2, the magnitude of $\Delta\Delta G^m_{unfold}$ was not significantly different from that of $\Delta\Delta G^0_{unfold}$ for all HEWL samples. Moreover, irrespective of the type of free energy change, the amount of free energy decrease from the control was positively correlated to the concentration of DTT^{red} added.

It has been reported that many proteins rely on disulfide bonds for the stability of their folded state and that reduction of the disulfide bonds will result in the unfolding of proteins (Creighton 1984; Oobatake et al. 1979). While the underlying mechanism is far from being completely understood, the stabilizing effect of disulfide bonds on proteins is believed to involve configurational entropic, enthalpic, and native-state effects (Betz 1993; Clarke and Fersht 1993). Apparently, the results of our unfolding experiments demonstrated that DTT^{red} interacted with HEWL, leading to a loss in conformational stability.

Table 2 Calculated urea-induced unfolding transition thermodynamic parameters of HEWL samples in presence and absence of DTT^{red} monitored by intrinsic fluorescence spectra

Sample	ΔG^0_{unfold} [a] (kJ/mol)	m_{unfold} [a] (kJ/mol-M)	C_m [a] (M)	$\Delta\Delta G^m_{unfold}$ [a] (kJ/mol)	$\Delta\Delta G^0_{unfold}$ [a] (kJ/mol)
HEWL	17.25 ± 0.48	3.09 ± 0.09	5.59 ± 0.04	–	–
HEWL + 1 mM DTT^{red}	15.13 ± 0.57	3.05 ± 0.12	4.97 ± 0.05	1.92 ± 0.12	2.11 ± 0.75
HEWL + 2 mM DTT^{red}	12.67 ± 0.33	3.11 ± 0.08	4.07 ± 0.04	4.72 ± 0.05	4.58 ± 0.59
HEWL + 4 mM DTT^{red}	10.12 ± 0.16	3.11 ± 0.05	3.26 ± 0.02	7.23 ± 0.04	7.13 ± 0.51

[a] The parameters were determined using the equations based on a two-state transition. Mechanism listed in the "Materials and methods" section

We also examined whether the addition of DTT^{red} could still inhibit the formation of HEWL fibrils once HEWL aggregation had commenced. After HEWL was allowed to aggregate in pH 2.0 at 55°C, we added 2 mM DTT^{red} at later time points (2, 5, and 8 days). As evidenced by ThT fluorescence results shown in Fig. 7a and Congo red binding (data not shown), the inhibitory effect of DTT^{red} was observed to be negatively correlated with the timing of DTT^{red} addition. Moreover, the addition of 2 mM DTT^{red} after ~8 days of incubation had no suppressing effect on either the rise in ThT fluorescence or the generation of the shoulder peak in Congo red binding spectra. By comparing against the spectra obtained from the control (HEWL by itself), our CD, intrinsic fluorescence, and ANS fluorescence results showed that the addition of DTT^{red} after ~8 days of incubation exerted negligible influence on the conformation (secondary or tertiary structure) of HEWL sample (see ANS data in Fig. 7b), in agreement with observations by ThT fluorescence and Congo red binding. Consequently, our findings demonstrated that DTT^{red} was effective in inhibiting HEWL fibrillation only when added within the period of partial unfolding (~8 days).

As inferred from our above-mentioned ThT fluorescence, light scattering, and equilibrium unfolding results, it is reasonable to postulate that, during the lag period of fibrillation, the addition of DTT^{red} drove the reaction to proceed through the off-pathway toward the formation of amorphous aggregates and decreased the effective concentration of HEWL for fibril formation, thus yielding significantly smaller amount of fibrils.

Among several models, the nucleation-based polymerization model, involving a lag period followed by a growth phase, has been widely used to account for the kinetics of amyloid fibrillation. It is thought that, during the lag period, the monomeric species assemble to form an oligomeric nucleus, which can serve as a template for subsequent fibrillation in the growth phase (Munishkina et al. 2004; Pedersen et al. 2004). Ample evidence has suggested that abnormal aggregation or fibrillation arises from a critical, partially unfolded protein intermediate (also known as the amyloidogenic intermediate) (Ohnishi and Takano 2004; Uversky and Fink 2004) and that this intermolecular association is driven by hydrophobic interactions (Khurana et al. 2003). The nucleus formed by the assembly of partially unfolded monomers possesses hydrophobic side-chains or patches on its surface, which leads to hydrophobic associations between the molecules and consequently the formation of fibril. Contrary to the partially unfolded intermediates, the fully unfolded and fully folded species lack the aforesaid hydrophobic side-chains; therefore, when they dominate the solution, inhibition or deceleration of fibrillation would be observed (Uversky and Fink 2004; Yagi et al. 2005). Given that the partial unfolding of HEWL occurred before ~8 days of incubation, it would be reasonable to surmise that, besides monomer, partially (un)folded intermediate conformation of HEWL might be still vulnerable to the action of DTT^{red} (e.g., reduction of the disulfide bond) or accessible to DTT^{red}, thus leading to the observed fibrillation inhibition. However, the lack of inhibitory potency against HEWL fibrillation by DTT^{red} detected afterwards might be attributed to the difficult access of DTT^{red} to the inner core of fibrils, as the aggregates are already tightly packed and assembled. A similar conclusion was also drawn from study examining the influence of reducing agents on β_2-microglobulin fibrillogenesis (Yamamoto et al. 2008). The possible explanation for our findings can be stated as follows: While the conditions of pH 2.0 and 55°C are suited for the generation of prerequisite partially folded intermediates for fibrillation, addition of DTT^{red} further unfolds the partially destabilized HEWL monomer and/or oligomeric nucleus species by reducing disulfide bridges, hence providing a condition favoring formation of fully unfolded population. The resultant extensive unfolding of HEWL generated predominantly amorphous aggregates (off-pathway product), with fewer fibrillar species (on-pathway product) being formed, which substantially delays or inhibits HEWL fibrillation.

Thiol-based redox pairs have commonly been added to the buffer to refold disulfide-containing proteins/peptides (De Bernardez Clark et al. 1998, 1999). Also, the redox buffer composition can affect in vitro folding rates and folding states of proteins (Bulaj 2005). Therefore, we were interested in knowing whether the presence of DTT^{ox} would influence

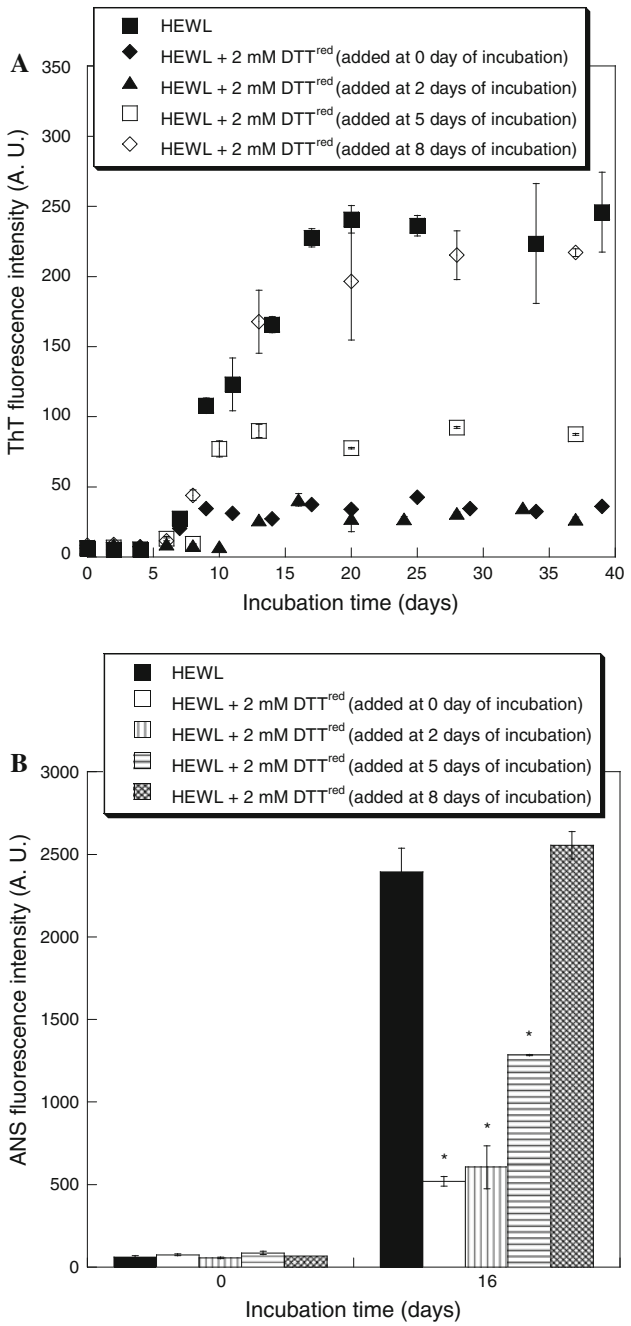

Fig. 7 Effect of timing of DTT^{red} addition on **a** the amyloid fibrillation and **b** the surface hydrophobicity of HEWL sample as a function of incubation time. The inhibitory effect of DTT^{red} on fibrillation of HEWL samples was evaluated by the time course of ThT fluorescence emission. ANS fluorescence emission was used to monitor the surface hydrophobicity of HEWL samples. HEWL samples were prepared in hydrochloric acid (pH 2.0) with salt at 55°C. DTT^{red} at 2 mM was added at different time points (0, 2, 5, and 8 days) after the launch of incubation. Each *point* represents the average of at least five independent measurements ($n \geq 5$). In Fig. 7b, an *asterisk* above the *bar* indicates that the statistical difference between the sample value and its untreated control value has a P value of <0.005 as determined by Student's t test

amyloid fibrillation of HEWL. As illustrated in Fig. 8a, when 2 mM DTT^{ox} was initially added to the HEWL sample, not much difference in final ThT fluorescence intensity was observed in comparison with that of HEWL by itself. However, when co-incubated with its reduced counterpart, DTT^{red}, dramatic declines of ThT fluorescence emissions in HEWL samples were perceived even over ~35 days of incubation. Furthermore, the far-UV CD spectra of HEWL by itself and of DTT^{red}-containing HEWL samples remained unaffected by the addition of DTT^{ox} (spectra not shown). A similar conclusion concerning the influence of DTT^{ox} (2 mM or 4 mM) could be drawn from observations of intrinsic fluorescence spectra (spectra not shown) and ANS fluorescence emission spectra (Fig. 8b). Our findings clearly indicated that the addition of oxidized DTT had no effects on the secondary and tertiary structures of HEWL. Moreover, the observed inhibitory activity against HEWL amyloid fibrillation induced by DTT^{red} was not confounded by supplementation with DTT^{ox}.

Based on the preceding results, we hypothesized that the destabilization of three-dimensional structure and the inhibition of HEWL fibrillation caused by DTT^{red} would be closely associated with the reduction of disulfide bridges of HEWL. To investigate this further, we proceeded to determine the content of free thiol groups (–SH) in HEWL samples under different conditions. We show in Table 3 that the acid-induced fibrillation of HEWL by itself led to a slight increase in –SH content (~0.032 mM) even after 25 days of incubation. However, the exposure of –SH groups was more pronounced in DTT^{red}-containing samples as compared with the control sample, and the free –SH concentration and percentage of native disulfide disruption were positively correlated with the added DTT^{red} concentration. For example, after 10 days of incubation, ~3.0%, ~28.2%, ~37.1%, and ~51.7% of eight thiol groups in HEWL appeared free for the HEWL samples with 0 mM, 1 mM, 2 mM, and 4 mM DTT^{red}, respectively. Except for the control sample, a decrease was observed at 25 days of incubation in each DTT^{red}-containing sample, as shown in Table 3. The decrease in thiol levels observed later was probably attributable to reformation of disulfide bonds either intra- or intermolecularly. An analogous trend was also observed in a previous study (Kumar et al. 2008).

A number of disulfide-bonded proteins such as insulin, α-synuclein, and cystatin C have been recognized as the fibrillar components of the deposits associated with certain diseases (Dobson 2004; Ross and Poirier 2004; Uversky and Fink 2004; Wang and Good 2005). Earlier studies provided evidence of the link between disulfide bonds and amyloid fibrillation. It was shown that, in familial British dementia, the intramolecular disulfide bridge is needed for

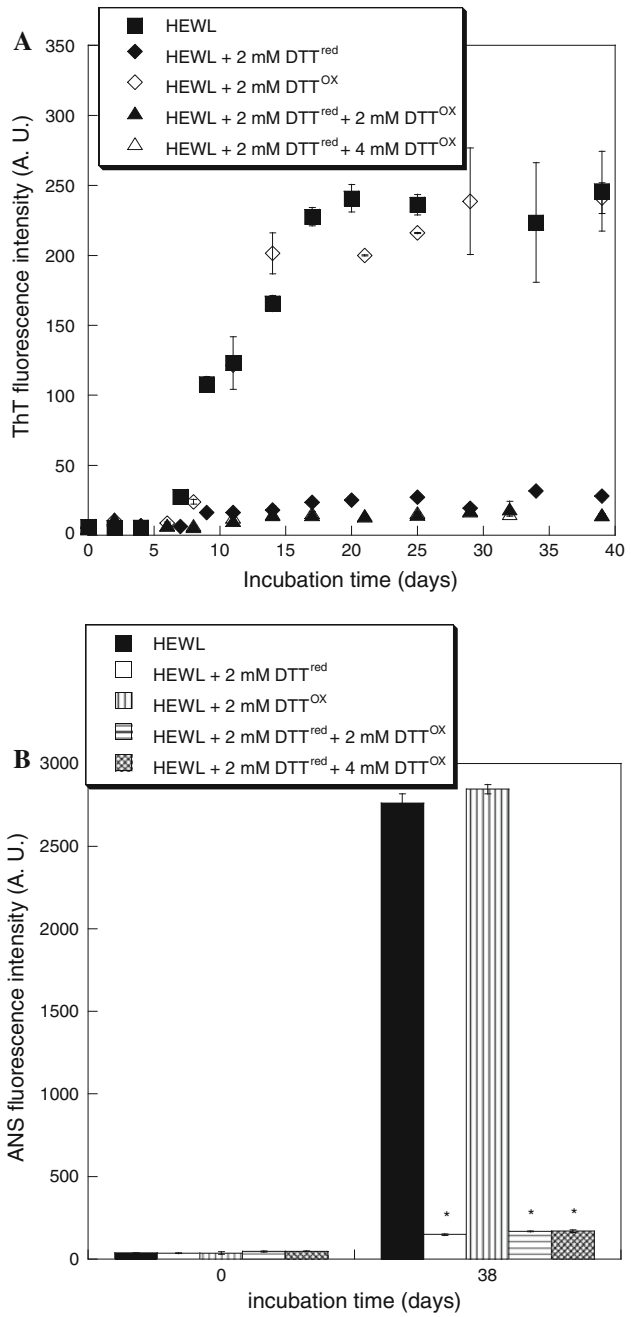

Fig. 8 Effect of DTT^{ox} on **a** the amyloid fibrillation and **b** the surface hydrophobicity of HEWL sample as a function of incubation time. Each *point* represents the average of at least five independent measurements ($n \geq 5$). HEWL samples were prepared in hydrochloric acid (pH 2.0) with salt in the presence of various concentrations of DTT^{ox} (0, 2 and 4 mM) with or without 2 mM DTT^{red}, and incubation was performed at 55°C. In Fig. 8b, an *asterisk* above the *bar* indicates that the statistical difference between the sample value and its untreated control value has a P value of <0.005 as determined by Student's t test

the generation of β-sheet-rich fibrils (El-Agnaf et al. 2001). Zhang and Kelly observed that transthyretin variant bearing Cys10 mixed disulfides has a higher propensity for fibrillation than its wild-type counterpart (Zhang and Kelly 2003). It has been demonstrated that a number of peptides/proteins containing native disulfide bonds are unable to form amyloid fibrils when the disulfide bonds are disrupted (Das et al. 2005; Thorn et al. 2008). Previously, a number of attempts have been made to investigate how amyloid fibrillation is affected by an added reducing agent. Using hemodialysis amyloidosis-associated protein, β_2-microglobulin, as a model protein, Yamamoto and coworkers reported that the addition of DTT or cysteine led to suppression of amyloid fibril formation at neutral pH (Yamamoto et al. 2008). Fibrillation of β_2-microglobulin was found to be hampered upon reduction of disulfide bonds under acidic condition (Ohhashi et al. 2002). Furthermore, our laboratory has recently demonstrated that the fibrillogenic propensity of hen egg-white lysozyme induced at low pH and elevated temperature was markedly attenuated due to the presence of tris(2-carboxyethyl) phosphine (TCEP), cysteine, or reduced glutathione (GSH) (Wang et al. 2009a, b, c). In stark contrast, the results from the study by Paik and coworkers revealed that, as compared with α-synuclein by itself, the addition of GSH profoundly increased the final emitted ThT fluorescence intensity (the amount of amyloid fibrils) without changing the lag period of fibrillation (Paik et al. 2003). While DTT^{red} has recently been shown to potently retard the slow aggregation of HEWL at pH 12.2 (Kumar et al. 2008), its effect on amyloid fibrillation of HEWL at acidic pH has not yet been reported.

Our data demonstrated that the level of exposed –SH groups was significantly low (~3% of eight free thiol) in the sample of HEWL by itself, indicating that disulfide bonds were present in HEWL without the addition of DTT^{red}. Moreover, no observable difference was detected in the percentage of free –SH before and after treatment of 6 M guanidine hydrochloride. It was previously reported that, after treating with reducing agents, both isolated A- and B-chain peptides of insulin have the propensity for fibrillation (Hong et al. 2006; Zako et al. 2009). In addition, Aso and coworkers have pointed out that the formation of both immature and mature fibrils could be observed even without the presence of any disulfide bond (Aso et al. 2007). Based on the results from us and others, we can reasonably conjecture that the existence of disulfide bonds is probably not a structural prerequisite for amyloid fibrillation.

In the present research, via fluorescence spectroscopy with ThT or ANS, circular dichroism spectroscopy, Congo red binding assay, and TEM, our results showed that DTT^{red} led to a marked reduction in HEWL fibrillation (Figs. 1, 2, 3). Moreover, subsequent experiments using HEWL treated with DTT^{red} at later times of incubation revealed that the effective inhibitory activity of DTT^{red} against HEWL fibrillation was noted only when DTT^{red}

Table 3 Concentrations and percentages of free thiol groups in HEWL samples with various concentrations of DTT^{red} after 10 or 25 days of incubation

$[DTT^{red}]$	0 mM	1 mM	2 mM	4 mM
[–SH] (mM) (10 days)	0.032 (~3%[a])	0.314 (~28%[a])	0.412 (~37%[a])	0.574 (~52%[a])
[–SH] (mM) (25 days)	0.032 (~3%[a])	0.260 (~24%[a])	0.388 (~35%[a])	0.412 (~37%[a])

[a] Numbers in parenthesis denote percentages of free thiol groups in HEWL samples, determined by the following formula: free thiol groups $\% = ([-SH])/([HEWL] \times 8)$

was added within ~8 days of incubation (Fig. 7). We then demonstrated that the inhibition of HEWL fibrillation was strongly dependent upon DTT^{red} but not DTT^{ox} (Fig. 8a). In terms of structure, ANS fluorescence emission spectra (not shown) and CD spectra were also recorded to monitor the changes in the surface hydrophobicity and secondary structure, respectively. We discovered that, as opposed to the β-sheet-rich amyloid fibrils with higher hydrophobicity formed in HEWL alone or DTT^{ox}-containing HEWL, species with predominately low β-sheet structure and lower solvent-exposed hydrophobic surfaces were detected in the HEWL samples with initial addition of DTT^{red} (Fig. 5a–c). Furthermore, the observed changes in structural feature induced by DTT^{red} were not disturbed by the presence of DTT^{ox} (Fig. 8b). It could be concluded from the results of ANS fluorescence, intrinsic fluorescence, urea-unfolding data, and free thiol measurements that the reducing environment or addition of DTT^{red} led to the reduction of disulfide bonds and thus enhanced the conformational flexibility of HEWL and decreased the stability of HEWL (Tables 1, 2, 3; Figs. 5, 6). As a result, partial loss of tertiary structure arose and tryptophan residues which were huddled inside become accessible to the solvent.

Notably, upon closer examination our data revealed that up to ~90% reduction in fibrillation was observed when only ~50% of disulfide bonds were disrupted by the addition of DTT^{red}. As stated above, others have found that amyloid fibrillation could be governed by formation of disulfide bonds inter- or intramolecularly (Das et al. 2005; Ohhashi et al. 2002; Welker et al. 2002). Alternatively, hydrophobic interaction was determined to be the key driving force for protein fibrillation (Shimizu and Shimizu 1999; Srisailam et al. 2002). Therefore, it could be postulated that the role played by the added DTT^{red} might be twofold: (1) breaking the disulfide bonds, and (2) rendering the structure or conformation of HEWL more flexible, thereby enhancing the exposure and solvent accessibility of the buried tryptophan residues, which may be associated with hydrophobic interactions.

In conclusion, we sought to explore the effects of dithiothreitol on amyloid fibril formation by investigating one of the best characterized systems, hen egg-white lysozyme. While additional studies are required on the effects of DTT^{red} on amyloid fibrillation to shed light on underlying mechanism(s), this study has revealed that the propensity for fibril formation of HEWL at acidic pH could be effectively suppressed by adding reductant (DTT^{red}), highlighting the importance of disulfide bridges in amyloid fibrillation. We believe that the outcome from this research will not only contribute to our understanding of the mechanism(s) regarding self-association of disease-relevant or disease-irrelevant amyloid proteins but also provide a promising approach to tackle the amyloid formation implicated in amyloid diseases.

Acknowledgments This work was supported by grants from the National Science Council, Taiwan. We are also grateful to the staffs of TC5 Bio-Image Tools, Technology Commons, College of Life Science, NTU for help with TEM.

References

Ahmad F, Taneja S, Yadav S, Haque SE (1994) A new method for testing the functional dependence of unfolding free-energy changes on denaturant concentration. J Biochem 115:322–327

Aso Y, Shiraki K, Takagi M (2007) Systematic analysis of aggregates from 38 kinds of non disease-related proteins: identifying the intrinsic propensity of polypeptides to form amyloid fibrils. Biosci Biotechnol Biochem 71:1313–1321

Bennett MC (2005) The role of alpha-synuclein in neurodegenerative diseases. Pharmacol Ther 105:311–331

Betz SF (1993) Disulfide bonds and the stability of globular-proteins. Protein Sci 2:1551–1558

Bliznyukov OP, Kozmin LD, Vysotskaya LL, Golenkov AK, Tishchenko VM, Samoylovich MP, Klimovich VB (2005) Human immunoglobulin light chains lambda form amyloid fibrils and granular aggregates in solution. Biochemistry-Moscow 70:458–466

Booth DR, Sunde M, Bellotti V, Robinson CV, Hutchinson WL, Fraser PE, Hawkins PN, Dobson CM, Radford SE, Blake CCF, Pepys MB (1997) Instability, unfolding and aggregation of human lysozyme variants underlying amyloid fibrillogenesis. Nature 385:787–793

Bulaj G (2005) Formation of disulfide bonds in proteins and peptides. Biotechnol Adv 23:87–92

Chen S, Berthelier V, Hamilton JB, O'Nuallai B, Wetzel R (2002) Amyloid-like features of polyglutamine aggregates and their assembly kinetics. Biochemistry 41:7391–7399

Chiti F, Dobson CM (2006) Protein misfolding, functional amyloid, and human disease. Annu Rev Biochem 75:333–366

Chiti F, Dobson CM (2009) Amyloid formation by globular proteins under native conditions. Nat Chem Biol 5:15–22

Clarke J, Fersht AR (1993) Engineered disulfide bonds as probes of the folding pathway of barnase—increasing the stability of proteins against the rate of denaturation. Biochemistry 32:4322–4329

Creighton TE (1984) Disulfide bond formation in proteins. Methods Enzymol 107:305–329

Dabora JM, Sanyal G, Middaugh CR (1991) Effect of polyanions on the refolding of human acidic fibroblast growth factor. J Biol Chem 266:23637–23640

Das AK, Drew MG, Haldar D, Banerjee A (2005) The role of the disulfide bond in amyloid-like fibrillogenesis in a model peptide system. Org Biomol Chem 3:3502–3507

De Bernardez Clark E (2001) Protein refolding for industrial processes. Curr Opin Biotechnol 12:202–207

De Bernardez Clark E, Hevehan D, Szela S, Maachupalli-Reddy J (1998) Oxidative renaturation of hen egg-white lysozyme. Folding vs aggregation. Biotechnol Progress 14:47–54

De Bernardez Clark E, Schwarz E, Rudolph R (1999) Inhibition of aggregation side reactions during in vitro protein folding. Methods Enzymol 309:217–236

Dobson CM (2004) Principles of protein folding, misfolding and aggregation. Semin Cell Dev Biol 15:3–16

El-Agnaf OM, Sheridan JM, Sidera C, Siligardi G, Hussain R, Haris PI, Austen BM (2001) Effect of the disulfide bridge and the C-terminal extension on the oligomerization of the amyloid peptide ABri implicated in familial British dementia. Biochemistry 40:3449–3457

Estrada LD, Soto C (2007) Disrupting beta-amyloid aggregation for Alzheimer disease treatment. Curr Top Med Chem 7:115–126

Fandrich M, Forge V, Buder K, Kittler M, Dobson CM, Diekmann S (2003) Myoglobin forms amyloid fibrils by association of unfolded polypeptide segments. Proc Natl Acad Sci USA 100:15463–15468

Ferrao-Gonzales AD, Souto SO, Silva JL, Foguel D (2000) The preaggregated state of an amyloidogenic protein: hydrostatic pressure converts native transthyretin into the amyloidogenic state. Proc Natl Acad Sci U S A 97:6445–6450

Frare E, de Laureto PP, Zurdo J, Dobson CM, Fontana A (2004) A highly amyloidogenic region of hen lysozyme. J Mol Biol 340:1153–1165

Gazova Z, Bellova A, Daxnerova Z, Imrich J, Kristian P, Tomascikova J, Bagelova J, Fedunova D, Antalik M (2008) Acridine derivatives inhibit lysozyme aggregation. Eur Biophys J 37:1261–1270

Goedert M, Spillantini MG (2006) A century of Alzheimer's disease. Science 314:777–781

Greene RF, Pace CN (1974) Urea and guanidine-hydrochloride denaturation of ribonuclease, lysozyme, alpha-chymotrypsin, and beta-lactoglobulin. J Biol Chem 249:5388–5393

Hong D-P, Ahmad A, Fink AL (2006) Fibrillation of human insulin A and B chains. Biochemistry 45:9342–9353

Kallberg Y, Gustafsson M, Persson B, Thyberg J, Johansson J (2001) Prediction of amyloid fibril-forming proteins. J Biol Chem 276:12945–12950

Kells DIC, O'Neil JDJ, Hofmann T (1984) A method for eliminating Rayleigh scattering from fluorescence spectra. Anal Biochem 139:316–318

Khurana R, Ionescu-Zanetti C, Pope M, Li J, Nielson L, Ramírez-Alvarado M, Regan L, Fink AL, Carter SA (2003) A general model for amyloid fibril assembly based on morphological studies using atomic force microscopy. Biophys J 85:1135–1144

Krebs MR, Wilkins DK, Chung EW, Pitkeathly MC, Chamberlain AK, Zurdo J, Robinson CV, Dobson CM (2000) Formation and seeding of amyloid fibrils from wild-type hen lysozyme and a peptide fragment from the beta-domain. J Mol Biol 300:541–549

Kumar S, Ravi VK, Swaminathan R (2008) How do surfactants and DTT affect the size, dynamics, activity and growth of soluble lysozyme aggregates? Biochem J 415:275–288

Lai Z, Colon W, Kelly JW (1996) The acid-mediated denaturation pathway of transthyretin yields a conformational intermediate that can self-assemble into amyloid. Biochemistry 35:6470–6482

Lansbury PT Jr (1999) Evolution of amyloid: what normal protein folding may tell us about fibrillogenesis and disease. Proc Natl Acad Sci U S A 96:3342–3344

Lee VM, Goedert M, Trojanowski JQ (2001) Neurodegenerative tauopathies. Annu Rev Neurosci 24:1121–1159

LeVine H 3rd (1993) Thioflavine T interaction with synthetic Alzheimer's disease beta- amyloid peptides: detection of amyloid aggregation in solution. Protein Sci 2:404–410

Liu CP, Li ZY, Huang GC, Perrett S, Zhou JM (2005) Two distinct intermediates of trigger factor are populated during guanidine denaturation. Biochimie 87:1023–1031

Mishra R, Sorgjerd K, Nystrom S, Nordigarden A, Yu YC, Hammarstrom P (2007) Lysozyme amyloidogenesis is accelerated by specific nicking and fragmentation but decelerated by intact protein binding and conversion. J Mol Biol 366:1029–1044

Morozova-Roche L, Malisauskas M (2007) A false paradise—mixed blessings in the protein universe: the amyloid as a new challenge in drug development. Curr Med Chem 14:1221–1230

Munishkina LA, Cooper EM, Uversky VN, Fink AL (2004) The effect of macromolecular crowding on protein aggregation and amyloid fibril formation. J Mol Recognit 17:456–464

Nakatani H, Maki K, Saeki K, Aizawa T, Demura M, Kawano K, Tomoda S, Kuwajima K (2007) Equilibrium and kinetics of the folding and unfolding of canine milk lysozyme. Biochemistry 46:5238–5251

Ohhashi Y, Hagihara Y, Kozhukh G, Hoshino M, Hasegawa K, Yamaguchi I, Naiki H, Goto Y (2002) The intrachain disulfide bond of beta(2)-microglobulin is not essential for the immunoglobulin fold at neutral pH, but is essential for amyloid fibril formation at acidic pH. J Biochem 131:45–52

Ohnishi S, Takano K (2004) Amyloid fibrils from the viewpoint of protein folding. Cell Mol Life Sci 61:511–524

Oobatake M, Takahashi S, Ooi T (1979) Conformational stability of ribonuclease-T1. 2. Salt-induced renaturation. J Biochem 86:65–70

Paik SR, Lee D, Cho H-J, Lee E-N, Chang C-S (2003) Oxidized glutathione stimulated the amyloid formation of [alpha]-synuclein. FEBS Lett 537:63–67

Pedersen JS, Christensen G, Otzen DE (2004) Modulation of S6 fibrillation by unfolding rates and gatekeeper residues. J Mol Biol 341:575–588

Pepys MB, Hawkins PN, Booth DR, Vigushin DM, Tennent GA, Soutar AK, Totty N, Nguyen O, Blake CC, Terry CJ et al (1993) Human lysozyme gene mutations cause hereditary systemic amyloidosis. Nature 362:553–557

Porat Y, Abramowitz A, Gazit E (2006) Inhibition of amyloid fibril formation by polyphenols: structural similarity and aromatic interactions as a common inhibition mechanism. Chem Biol Drug Des 67:27–37

Powers ET, Powers DL (2008) Mechanisms of protein fibril formation: Nucleated polymerization with competing off-pathway aggregation. Biophys J 94:379–391

Privalov PL (1996) Intermediate states in protein folding. J Mol Biol 258:707–725

Rodionova NA, Semisotnov GV, Kutyshenko VP, Uverskii VN, Bolotina IA (1989) Staged equilibrium of carbonic anhydrase unfolding in strong denaturants. Mol Biol (Mosk) 23:683–692

Ross CA, Poirier MA (2004) Protein aggregation and neurodegenerative disease. Nat Med 10(Suppl):S10–S17

Sasahara K, Demura M, Nitta K (2002) Equilibrium and kinetic folding of hen egg-white lysozyme under acidic conditions. Proteins-Struc Funct Genet 49:472–482

Semisotnov GV, Rodionova NA, Razgulyaev OI, Uversky VN, Gripas AF, Gilmanshin RI (1991) Study of the "molten globule" intermediate state in protein folding by a hydrophobic fluorescent probe. Biopolymers 31:119–128

Serpell LC, Sunde M, Benson MD, Tennent GA, Pepys MB, Fraser PE (2000) The protofilament substructure of amyloid fibrils. J Mol Biol 300:1033–1039

Shimizu S, Shimizu K (1999) Alcohol denaturation: thermodynamic theory of peptide unit solvation. J Am Chem Soc 121:2387–2394

Shtilerman MD, Ding TT, Lansbury PT Jr (2002) Molecular crowding accelerates fibrillization of alpha-synuclein: could an increase in the cytoplasmic protein concentration induce Parkinson's disease? Biochemistry 41:3855–3860

Singh SM, Panda AK (2005) Solubilization and refolding of bacterial inclusion body proteins. J Biosci Bioeng 99:303–310

Sirangelo I, Bismuto E, Tavassi S, Irace G (1998) Apomyoglobin folding intermediates characterized by the hydrophobic fluorescent probe 8-anilino-1-naphthalene sulfonate. Biochim Biophys Acta 1385:69–77

Smoot AL, Panda M, Brazil BT, Buckle AM, Fersht AR, Horowitz PM (2001) The binding of bis-ANS to the isolated GroEL apical domain fragment induces the formation of a folding intermediate with increased hydrophobic surface not observed in tetradecameric GroEL. Biochemistry 40:4484–4492

Srisailam S, Kumar TKS, Srimathi T, Yu C (2002) Influence of backbone conformation on protein aggregation. J Am Chem Soc 124:1884–1888

Srisailam S, Kumar TKS, Rajalingam D, Kathir KM, Sheu H-S, Jan F-J, Chao P-C, Yu C (2003) Amyloid-like Fibril formation in an all β-barrel protein. J Biol Chem 278:17701–17709

Taylor JP, Hardy J, Fischbeck KH (2002) Toxic proteins in neurodegenerative disease. Science 296:1991–1995

Thakur AK, Rao CM (2008) UV-light exposed prion protein fails to form amyloid fibrils. PLoS ONE 3:e2688

Thorn DC, Ecroyd H, Sunde M, Poon S, Carver JA (2008) Amyloid fibril formation by bovine milk alpha s2-casein occurs under physiological conditions yet is prevented by its natural counterpart, alpha s1-casein. Biochemistry 47:3926–3936

Uversky VN, Fink AL (2004) Conformational constraints for amyloid fibrillation: the importance of being unfolded. Biochim Biophys Acta 1698:131–153

Vaney MC, Maignan S, Ries-Kautt M, Ducriux A (1996) High-resolution structure (1.33 A) of a HEW lysozyme tetragonal crystal grown in the APCF apparatus. Data and structural comparison with a crystal grown under microgravity from SpaceHab-01 mission. Acta Crystallogr D Biol Crystallogr 52:505–517

Vetri V, Canale C, Relini A, Librizzi F, Militello V, Gliozzi A, Leone M (2007) Amyloid fibrils formation and amorphous aggregation in concanavalin A. Biophys Chem 125:184–190

Wang W (2005) Protein aggregation and its inhibition in biopharmaceutics. Int J Pharm 289:1–30

Wang SSS, Good TA (2005) An overview of Alzheimer's disease. J Chin Inst Chem Eng 36:533–559

Wang SSS, Chou SW, Liu KN, Wu CH (2009a) Effects of glutathione on amyloid fibrillation of hen egg-white lysozyme. Int J Biol Macromol 45:321–329

Wang SSS, Liu KN, Lu YC (2009b) Amyloid fibrillation of hen egg-white lysozyme is inhibited by TCEP. Biochem Biophys Res Commun 381:639–642

Wang SSS, Liu KN, Wu CH, Lai JK (2009c) Investigating the influences of redox buffer compositions on the amyloid fibrillogenesis of hen egg-white lysozyme. Biochimica Et Biophysica Acta-Proteins Proteomics 1794:1663–1672

Welker E, Raymond LD, Scheraga HA, Caughey B (2002) Intramolecular versus intermolecular disulfide bonds in prion proteins. J Biol Chem 277:33477–33481

Yagi H, Kusaka E, Hongo K, Mizobata T, Kawata Y (2005) Amyloid fibril formation of α-synuclein is accelerated by preformed amyloid seeds of other proteins. J Biol Chem 280:38609–38616

Yamamoto K, Yagi H, Ozawa D, Sasahara K, Naiki H, Goto Y (2008) Thiol compounds inhibit the formation of amyloid fibrils by [beta]2-microglobulin at neutral pH. J Mol Biol 376:258–268

Zako T, Sakono M, Hashimoto N, Ihara M, Maeda M (2009) Bovine insulin filaments induced by reducing disulfide bonds show a different morphology, secondary structure, and cell toxicity from intact insulin amyloid fibrils. Biophys J 96:3331–3340

Zhang QH, Kelly JW (2003) Cys10 mixed disulfides make transthyretin more amyloidogenic under mildly acidic conditions. Biochemistry 42:8756–8761

Zhu M, Souillac PO, Ionescu-Zanetti C, Carter SA, Fink AL (2002) Surface-catalyzed amyloid fibril formation. J Biol Chem 277:50914–50922